Heliyon 6 (2020) e03862

Contents lists available at ScienceDirect

Heliyon

journal homepage: www.cell.com/heliyon

Research article

Antineoplastic activity of a novel ruthenium complex against human hepatocellular carcinoma (HepG2) and human cervical adenocarcinoma (HeLa) cells

Carlos Eduardo Alves de Souza [a], Amanda do Rocio Andrade Pires [b], Carolina Riverin Cardoso [c], Rose Maria Carlos [c], Silvia Maria Suter Correia Cadena [b], Alexandra Acco [a,*]

[a] Department of Pharmacology, Federal University of Parana, Curitiba, Brazil
[b] Department of Biochemistry and Molecular Biology, Federal University of Parana, Curitiba, Brazil
[c] Department of Chemistry, Federal São Carlos University, São Carlos, Brazil

ARTICLE INFO

Keywords:
Biochemistry
Toxicology
Pharmaceutical chemistry
Pharmacology
Oncology
Hepatocellular carcinoma
Metabolism
HepG2 cells
Ruthenium complex
HeLa cells: Cell respiration

ABSTRACT

Novel metal complexes have received much attention recently because of their potential anticancer activity. Notably, ruthenium-based complexes have emerged as good alternatives to the currently used platinum-based drugs for cancer therapy, with less toxicity and fewer side effects. The beneficial properties of Ru, which make it a highly promising therapeutic agent, include its variable oxidative states, low toxicity, and high selectivity for cancer cells. The present study evaluated the cytotoxic effects of a ruthenium complex, namely *cis*-$[Ru(1,10\text{-phenanthroline})_2(imidazole)_2]^{2+}$ (RuC), on human hepatocellular carcinoma (HepG2) and human cervical adenocarcinoma (HeLa) cells and analyzed metabolic parameters. RuC reduced HepG2 and HeLa cell viability at all tested concentrations (10, 50, and 100 nmol/L) at 48 h of incubation, based on the MTT, Crystal violet, and neutral red assays. The proliferation capacity of HepG2 cells did not recover, whereas HeLa cell proliferation partially recovered after RuC treatment. RuC also inhibited all states of cell respiration and increased the levels of the metabolites pyruvate and lactate in both cell lines. The cytotoxicity of RuC was higher than cisplatin (positive control) in both lineages. These results indicate that RuC affects metabolic functions that are related to the energy provision and viability of HepG2 and HeLa cells and is a promising candidate for further investigations that utilize models of human cervical adenocarcinoma and mainly hepatocellular carcinoma.

1. Introduction

Cancer is among the principal causes of morbidity and mortality worldwide. The World Health Organization projects an increase in the number of new cancer cases over the next two decades, reaching 29.5 million people [1]. Chemotherapy is the most frequent treatment for cancer patients. Metals, particularly transition metals that have a wide structural diversity offer potential advantages over the more common organic-based drugs [2]. Cisplatin is a well-known metal drug that has been used in oncology since the 1970s [3]. Cisplatin has been a frequent choice for the treatment of a wide range of cancers, including ovarian, testicular, head and neck, bladder, and lung cancer [4]. However, the efficacy of cisplatin is limited by acquired or intrinsic resistance and severe side effects, such as ototoxicity, peripheral neuropathy, myelosuppression, and nephrotoxicity [5]. Consequently, novel metal anti-cancer compounds have been synthesized with the goal of discovering more efficient drugs with fewer side effects. Ruthenium (Ru) organometallic complexes have been synthesized as an alternative to cisplatin treatment. These complexes are considered pro-drugs because they are only effective against tumor cells after the reduction of Ru(III) to Ru(II) by biological reducing agents [6, 7, 8, 9]. Electrochemical experiments have shown that this reduction is favored in solid tumors compared with healthy tissue because of the low oxygen concentration (i.e., hypoxia) and acidic pH in the tumor microenvironment [10, 11, 12].

The compound *cis*-$[Ru(phen)_2(ImH)_2]^{2+}$, referred to as RuphenImH or RuC (Figure 1), has important cytotoxic effects compared with cisplatin against colorectal adenocarcinoma HT116 cells ($p53^{-/-}$) and HT116 cells ($p53^{+/+}$). RuC promoted cell cycle arrest in the G1 phase, which was more pronounced in HT116 cells ($p53^{+/+}$) [13]. In HT116

* Corresponding author.
E-mail address: aleacco@ufpr.br (A. Acco).

https://doi.org/10.1016/j.heliyon.2020.e03862
Received 22 January 2019; Received in revised form 21 May 2019; Accepted 22 April 2020

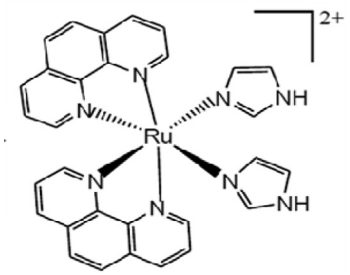

Figure 1. Chemical structure of RuC (*cis*-$[Ru(1,10\text{-phen})_2(ImH)_2]^{2+}$), based on International Union of Pure and Applied Chemistry nomenclature, in which *phen* refers to 1,10-phenanthroline and *ImH* refers to imidazole.

cells ($p53^{+/+}$), RuC was unable to induce the cleavage of caspase 3 and poly (ADP-ribose) polymerases (PARPs), suggesting that apoptosis was not involved in the inhibition of cell proliferation. We recently showed that RuC was effective against Walker-256 tumors in rats through the modulation of oxidative stress and impairment of oxidative phosphorylation, resulting in necrosis rather than apoptosis in these tumor cells [14]. Additionally, no clinical signs of toxicity or death were observed in rats that were treated for two weeks with RuC [14].

Cancer cells exhibit alterations of metabolism to maintain their rapid growth and proliferation. They depend on the synthesis of adenosine triphosphate (ATP) by glycolysis rather than oxidative phosphorylation, a phenomenon that is known as the Warburg effect [15]. This effect was first attributed to mitochondrial dysfunction, but this mechanism has been reconsidered [16]. In fact, in cancer cell mitochondria, anaplerotic and cataplerotic reactions work together to provide sufficient biosynthetic precursors, supporting cell proliferation. Thus, in contrast to Warburg's earliest observations, the maintenance of functional mitochondria appears to be essential for the survival and proliferation of cancer cells [17, 18]. The present study investigated this metabolic approach. We first evaluated the toxicity of RuC in different cell lines, including human hepatocarcinoma (HepG2) cells, cervical adenocarcinoma (HeLa) cells, glioblastoma (U87MG) cells, triple negative breast adenocarcinoma (MDA-MB-231) cells, hormone positive breast adenocarcinoma cell line (MCF-7), murine melanoma (B16F10) cells and non-tumor human embryonic kidney (HEK293) cells. We then investigated the cytotoxicity of RuC in HepG2 and HeLa cells that is associated with metabolic changes in both cell lines. The inhibition of respiration and activation of anaerobic glycolysis that were induced by RuC make it a promising alternative for the treatment of HCC and cervical adenocarcinoma, with the advantage of minimizing the adverse effects that are caused by other transition metals.

2. Materials and methods

2.1. Chemicals

High-glucose Dulbecco's modified Eagle's medium (DMEM HG) and Minimum Essential Medium (MEM) were obtained from Cultilab (Campinas, SP, Brazil). Fetal bovine serum (FBS) was purchased from Cripion Biotechnology (Andradina, SP, Brazil). Dimethylsulfoxide (DMSO) was obtained from Merck (São Paulo, SP, Brazil). Bovine serum albumin (BSA), 3-(4,5-dimethythiazol-2-yl)-2,5-diphenyltetrazolium bromide (MTT), 4-(2-hydroxyethyl)-1-piperazine ethanesulfonic acid (HEPES), and Trypan blue were purchased from Sigma. *cis*-Diamineplatinum(II) dichloride (cisplatin) was obtained from Sigma-Aldrich with a ≥99.9% trace metal basis. Ruthenium complex (*cis*-$[Ru(phen)_2(ImH)_2]^{2+}$; also called RuphenImH or RuC; Figure 1) was synthesized by the Department of Chemistry, Federal University of São Carlos, São Paulo, Brazil, and its structure was confirmed by ^{1}H NMR, ^{13}C NMR, and mass spectrometry according to Cardoso et al. [13]. In the present study, the compound was dissolved in DMSO and then further diluted with the assay medium. Controls with DMSO (0.1%, v/v) were included for each assay. All of the other reagents were commercial products of the highest available grade of purity.

2.2. Cell culture

HepG2, U87MG, and MDA-MB-231 cells were maintained in DMEM HG. HeLa cells were maintained in MEM. HEK293 and B16F10 cells were maintained in RPMI medium. All of the cell lines were obtained from the American Type Culture Collection. The culture media were supplemented with 10% FBS, 100 UI/mL penicillin G, 100 μg/mL streptomycin, and 20 mmol/L HEPES, adjusted to pH 7.4 with 1 mol/L sodium bicarbonate. HepG2 cells were grown in poly-L-lysine-coated flasks at 37 °C in 5% CO_2 with controlled humidity. Subculturing was performed at approximately 48 h intervals, and cell growth was monitored with an Olympus inverted microscope.

2.3. Toxicity screening of RuC

To establish the range of RuC concentrations, the sensitivity of the cell lines, and treatment times, toxicity assays were performed at RuC concentrations of 10 nmol/L to 1000 nmol/L in several tumor cell lines (HeLa, HepG2, B16F10, U87MG, and MDA-MB-231) and in the HEK293 immortalized kidney cell line. The cells were treated with RuC for 24, 48, and 72 h, and cell viability was evaluated by the MTT method as described below. For comparison, the cells were also treated with cisplatin (1–20 μmol/L) or DMSO (0.1%, v/v) in each assay as positive and negative controls, respectively.

2.4. Cytotoxicity assays

The treatment conditions were defined based on the results of the screening assays. HepG2 and HeLa cells were treated with cisplatin (5 and 10 μmol/L) and RuC (10, 50, and 100 nmol/L) for 48 h.

2.4.1. MTT assay

The cells (1×10^4 cells/well) were seeded in 96-well culture plates and after 24 h (confluent state of ~70%) were treated with cisplatin and RuC. After treatment, 200 μL of MTT solution (0.5 mg/mL) was added to each well and incubated for 3 h at 37 °C. The culture medium was discarded and 200 μL of DMSO solution was added to each well [19, 20]. The absorbance of formazan was read at 570 nm in a microplate reader (TECAN Infinite Reader, Männedorf, Switzerland). The results are expressed as a percentage of viable cells compared with controls (taken as 100%).

2.4.2. Crystal violet assay

The Crystal violet assay was performed according to Gillies, Didier and Denton [21]. Cells were seeded in culture plates. After 24 h, they were treated with cisplatin or RuC. The cell monolayer was then washed with PBS and fixed with 100 μL of cold absolute methanol for 10 min. The cells were stained with Crystal violet dye solution (0.2% Crystal violet, 2% ethanol) for 3 min and successively washed with PBS to remove excess dye. The remaining dye was solubilized with Crystal violet destaining solution (50% ethanol, 0.05 M sodium citrate), and absorbance was read at 540 nm in a microplate reader (TECAN Infinite Reader, Männedorf, Switzerland).

2.4.3. Neutral red assay

Cells (1×10^4 cells per well) were plated on 96-well plates. After 24 h, they were treated with cisplatin or RuC. After 48 h of incubation, the medium was removed, and the cells were washed twice with 150 μL of PBS solution per well heated at 37 °C. The neutral red assay was performed according to Borenfreund and Puerner [22]. The cells were flooded with 100 μL of neutral red solution (50 μg/mL neutral red in the culture medium) and incubated for 4 h at 37 °C in a 5% CO_2 atmosphere.

The neutral red solution was then discarded, and the cells were washed twice with 150 μL of PBS and 150 μL of fixative solution (1% formaldehyde, 1% calcium chloride) for 2 min. The plates were then rapidly drained, followed by the addition of 200 mL of extraction buffer (1% acetic acid and 50% ethanol) and left in the dark for 20 min at room temperature. The absorbance of the extracted dye was read at 570 nm in a microplate reader (TECAN Infinite Reader, Männedorf, Switzerland).

2.5. Cell proliferation

HepG2 and HeLa cells were plated on 96-well plates at a density of 1 $\times$ 10^4 cells per well at a final volume of 200 μL. Cell proliferation at 24, 48, and 72 h was determined by the Crystal violet method described above.

2.6. Cell respiration

HepG2 and HeLa cells were grown on a 60 mm plate and treated with RuC (10, 50, and 100 nmol/L) or cisplatin (5 and 10 μmol/L) for 48 h. After treatment, the cells were removed with trypsin and resuspended in DMEM HG or MEM for HepG2 and HeLa cells, respectively, and cell viability was assessed by the Trypan blue dye exclusion assay [23] in a Neubauer chamber. Cell respiration was then measured by high-resolution respirometry using an Oxygraph-2k device (Oroboros Instruments, Innsbruck, Austria) in two chambers at 37 °C with gentle agitation. Cell respiration (10^6 viable cells/chamber) was monitored in DMEM HG or MEM for HepG2 or HeLa cells, respectively. Oxygen flux was determined in the different states of respiration as previously described [24, 25, 26, 27]. These states were defined as *basal* (oxygen consumption in the absence of inhibitors or uncouplers), *leak* (respiration in the presence of 2 μg/mL oligomycin, which results in the reentry of protons into the mitochondrial matrix and represents respiration that is not coupled to ATP synthesis), and *uncoupled* (oxygen consumption in the presence of 0.5 μmol/L carbonyl cyanide-4-[trifluoromethoxy] phenylhydrazone [FCCP], corresponding to the maximal respiratory capacity to restore the dissipated proton gradient that is caused by the presence of the uncoupling agent). The oxygen flow in these states was corrected by subtracting non-mitochondrial respiration, which was obtained after the addition of rotenone (0.5 μmol/L) and antimycin (3 μg/mL). The results were analyzed using DataLab4 software and are expressed as the mean ± standard error of the mean (SEM) of cell oxygen flow (pmol·[seg $\times$ 10^6 cells]$^{-1}$).

2.7. Determination of lactate and pyruvate released by cultured cells

HepG2 and HeLa cells were cultured in DMEM HG and MEM, respectively, and treated for 48 h with cisplatin (5 and 10 μmol/L) and RuC (10, 50, and 100 nmol/L). The supernatant was then collected and centrifuged at 1500 rotations per minute for 5 min. Finally, the concentrations of lactate and pyruvate in the supernatant were measured as previously described [28, 29].

2.8. Proliferation recovery curve of HepG2 and HeLa cells

Cell proliferation recovery curves were constructed for both cell lines, which were seeded in six-well plates at a density of 1.5 $\times$ 10^4 in a final volume of 1 mL. After 24 h of plating, the number of cells was determined (day 1) by Trypan blue method, and another set of plates was treated with cisplatin (100 nmol/L, 5 μmol/L, and 10 μmol/L) or RuC (10, 50, and 100 nmol/L) for 48 h (day 3). After this time, the treatment was removed, the wells were washed with 500 μL of PBS, and the culture medium was replaced every 2 days. The HepG2 were maintained in DMEM HG and HeLa cells in MEM, both at 37 °C in 5% CO_2 with controlled humidity. Cell viability was determined by Trypan blue method every 2 days for 9 days (day 5 to day 9), and the results are expressed as the number of viable cells ($\times$ 10^4/mL).

2.9. Protein determination

The cell protein concentrations were determined using the Bradford method, with BSA as the standard [30], and used when necessary to normalize the amount of protein in assays of cultured cells.

2.10. Statistical analysis

The statistical analysis was performed using the Shapiro-Wilk normality test, one-way analysis of variance (ANOVA) followed by the Tukey *post hoc* test, or two-way ANOVA followed by the Bonferroni test when comparing cellular proliferation curves. The results are expressed as mean ± SEM. Values of $p < 0.05$ were considered statistically significant. The inhibitory concentrations 50% (IC_{50}) were calculated by nonlinear regression using log(inhibitor) *versus* normalized response curves in the GraphPad Prism 6.0 software (San Diego, CA, USA).

3. Results

3.1. RuC toxicity screening in different cell lines

The RuC complex, at a range of concentrations from 10 nmol/L to 1000 nmol/L, reduced the viability of all cell lines beginning at 24 h of treatment to the maximum treatment time of 72 h (Supplementary Tables S1 and S2, respectively). As shown in Table 1, after 48 h of treatment, RuC was more cytotoxic in HepG2, MCF-7 and HeLa cells, with inhibitory concentrations (IC_{50}) of 47.56, 62.82 and 230.3 nmol/L, respectively. Interestingly, the non-tumor cell line HEK293 was less affected than the tumor cell lines, particularly at 48 h of treatment, with an IC_{50} of 1370 nmol/L. Considering these results and the consistency of the data along the time-course of the experiment in the cell lines that were tested, HepG2 and HeLa cells were chosen for the subsequent experiments. RuC concentrations of 10, 50, and 100 nmol/L and a treatment time of 48 h were used, and cisplatin (5 and 10 μmol/L) was included as a positive control.

The cell lines were treated with RuC at concentrations of 10 nmol/L to 1 μmol/L for 48 h. The experimental conditions are described in the Materials and Methods. Briefly, the cells (10^4 cells/well) were seeded in 96-well plates with RuC and incubated for 48 h. Cell viability was evaluated by the MTT assay. The results are represented as the viability of the control (100% in the absence of RuC) and are expressed as the mean ± SEM of four independent experiments each in triplicate; n = 12. The IC_{50} was calculated using GraphPad Prism 6.0 software.

3.2. RuC is toxic in HepG2 and HeLa cells

The RuC complex (10, 50, and 100 nmol/L) and cisplatin (5 and 10 μmol/L) were toxic in both cell lines after 48 h of treatment. Viability was evaluated by the MTT assay. Viability decreased by 38% and 42% in HepG2 cells and by 63% and 28% in HeLa cells at the highest concentrations of RuC (100 nmol/L) and cisplatin (10 μmol/L), respectively (Figure 2A, B). The MTT assay is based on the activity of cellular dehydrogenases, and we also performed viability assays using crystal violet and neutral red to confirm the results. Crystal violet stains the nucleus of fixed cells, which are considered viable. Neutral red stains acidic vesicles in cells during the process of cell death. The determination of cell viability by crystal violet staining revealed 60% and 28% reductions of HepG2 cell viability and 33% and 51% reductions of HeLa cell viability at the highest concentrations of RuC (100 nmol/L) and cisplatin (10 μmol/L), respectively (Figure 2C, D). The same effect was observed in the neutral red assay, in which RuC and cisplatin at the same concentrations

Table 1. Toxicity of RuC complex in different cell lines, indicated by cell viability (%) and the IC_{50} (nmol/L) after 48 h of exposure.

Cell line	Cell viability (% of control)								IC_{50} (nmol/L)
	RuC concentration								
	10 nmol/L	50 nmol/L	100 nmol/L	200 nmol/L	400 nmol/L	600 nmol/L	800 nmol/L	1000 nmol/L	
HEK 293	82.3 ± 9.2	87.4 ± 6.8	72.3 ± 9.1	74.1 ± 1.3	82.3 ± 3.5	67.1 ± 6.8	64.3 ± 6.6	68.6 ± 4.3	1370
HepG2	95.0 ± 3.1	61.8 ± 3.6	60.8 ± 2.1	41.3 ± 5.0	43.8 ± 5.1	33.1 ± 3.9	34.0 ± 2.6	39.5 ± 6.7	47.56
HeLa	69.3 ± 2.3	53.0 ± 4.4	37.0 ± 0.7	20.3 ± 1.6	6.4 ± 0.2	6.4 ± 0.8	6.2 ± 0.2	6.3 ± 1.1	230.30
B16F10	104.9 ± 9.9	97.1 ± 0.1	95.0 ± 14.6	91.9 ± 3.7	81.0 ± 3.1	83.1 ± 1.1	83.9 ± 1.8	80.3 ± 10.4	3297
U87MG	74.1 ± 4.6	75.9 ± 3.5	71.3 ± 3.5	82.4 ± 8.9	80.0 ± 5.5	67.6 ± 0.8	71.8 ± 1.3	69.2 ± 1.5	1531
MDA-MB-231	59.6 ± 5.5	60.3 ± 5.7	44.1 ± 5.8	37.0 ± 7.3	53.2 ± 3.4	38.4 ± 5.1	49.2 ± 2.8	41.8 ± 2.8	230.40
MCF-7	42.8 ± 6.9	38.3 ± 2.2	35.5 ± 9.3	34.6 ± 1.0	32.6 ± 5.1	36.7 ± 4.4	35.9 ± 4.3	36.9 ± 3.0	62.82

reduced HepG2 cell viability by 48% and 74% and reduced HeLa cell viability by 38% and 58%, respectively (Figure 2E, F).

3.3. RuC affects HepG2 and HeLa cell proliferation

The crystal violet data were used to plot a cell proliferation curve of the activity of cellular dehydrogenases at 24, 48, and 72 h. A gradual reduction of cell proliferation was observed after 48 and 72 h of treatment, with the exception of the control condition. Cell proliferation exhibited a time-dependent decline at both concentrations of cisplatin (10 μmol/L) and at the highest concentrations of RuC (50 and 100 nmol/L) in both HepG2 (Figure 3A) and HeLa (Figure 3B) cells.

3.4. RuC affects the respiration of HepG2 and HeLa cells

Considering the significant reductions of cell viability and proliferation, we evaluated the effects of RuC and cisplatin on the respiration of HepG2 and HeLa cells. These assays were performed using non-

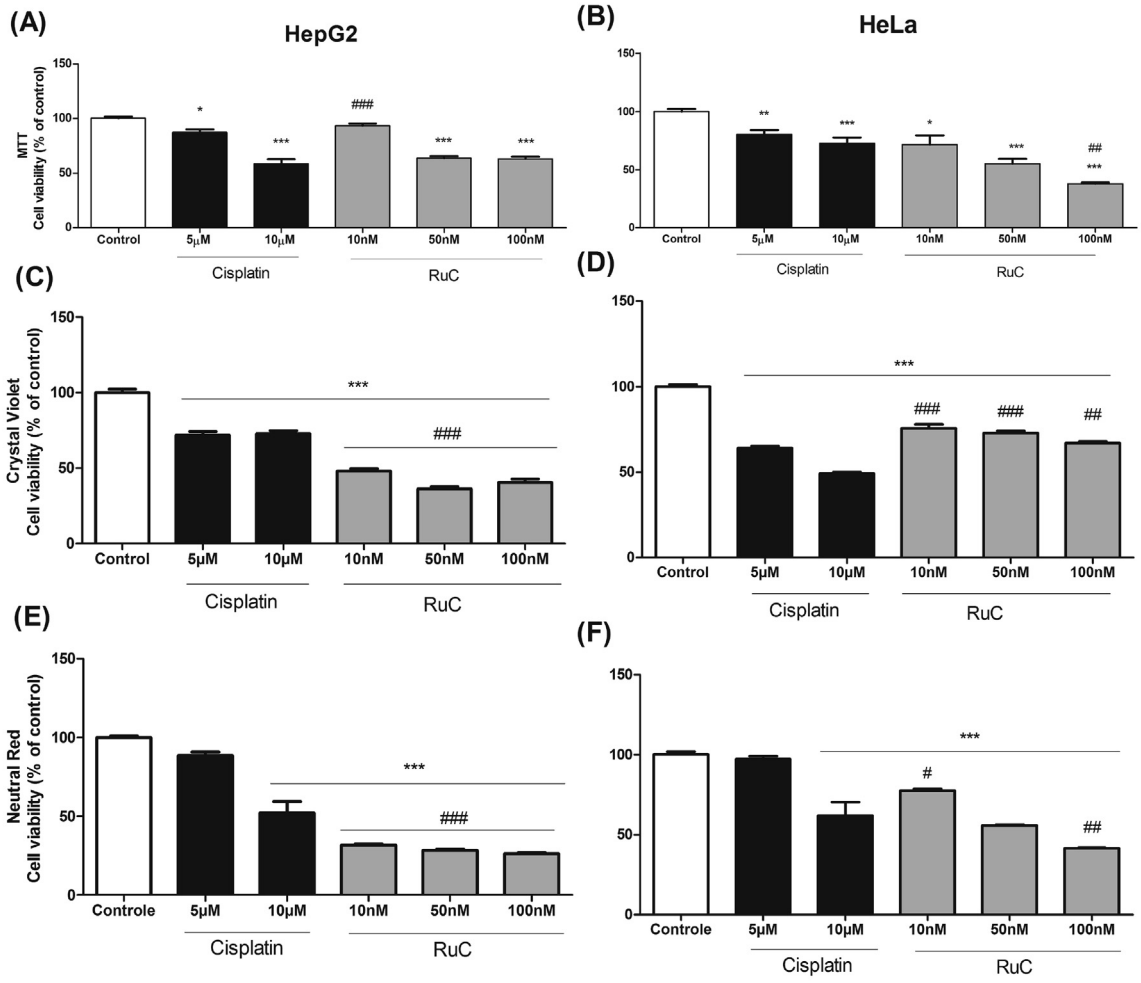

Figure 2. Cytotoxicity of cisplatin and RuC in HepG2 and HeLa cells, revealed by the MTT (A, B), crystal violet (C, D), and neutral red (E, F) assays. The experimental conditions are described in the Materials and Methods. Briefly, the cells (10^4 cells/well) were seeded in 96-well plates with cisplatin (5 and 10 μmol/L) or RuC (10, 50, and 100 nmol/L) for 48 h. The values are expressed as the mean ± SEM of six independent experiments each in triplicate; n = 18. The results are expressed as a percentage of control (0.1% DMSO). $^{*}p < 0.05$, $^{**}p < 0.01$, $^{***}p < 0.001$, significantly different from control; $^{\#}p < 0.05$, $^{\#\#}p < 0.01$, $^{\#\#\#}p < 0.001$, significantly different from 10 μmol/L cisplatin.

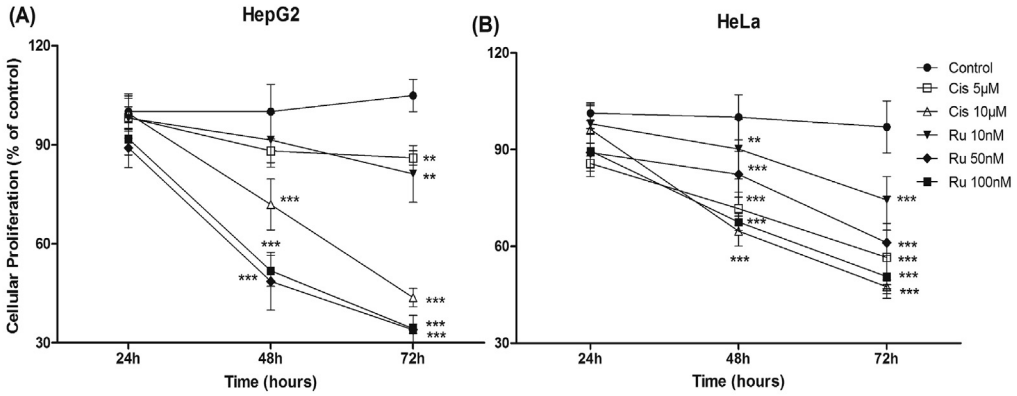

Figure 3. Effect of RuC and cisplatin on the proliferation of HepG2 (A) and HeLa (B cells. The experimental conditions are described in the Materials and Methods. The cells were cultured for 48 h before the addition of cisplatin (100 nmol/L, 5 μmol/L, and 10 μmol/L) or RuC (10, 50, and 100 nmol/L).). The values are expressed as the mean ± SEM of six independent experiments each in quadruplicate; n = 24. The crystal violet results are expressed as a percentage of control (0.1% DMSO) at 24 h. $*p < 0.05$, $**p < 0.01$, $***p < 0.001$, significantly different from control at the same time of treatment.

permeabilized cells in an attempt to approximate the experimental conditions to physiological conditions. Figure 4 shows cell respiration after 48 h of drug treatment. In HepG2 cells, the highest concentrations of RuC inhibited the basal state by 77% (Figure 4A), the leak state by 62% (Figure 4C), and the uncoupled state by 86% (Figure 4E). Interestingly, both concentrations of cisplatin (5 and 10 μmol/L) did not alter the respiration of these cells.

In HeLa cells, the basal and uncoupled states were inhibited by both drugs (Figure 4B, F). The basal state was inhibited by 5 and 10 μmol/L cisplatin (62% and 72%). RuC inhibited the basal state by 84%, 85%, and 91% at concentrations of 10, 50, and 100 nmol/L, respectively (Figure 4B). Only the highest concentration of RuC (100 nmol/L) inhibited the leak state by 61% (Figure 4D). The uncoupled state was inhibited by 91% by all concentrations of cisplatin and RuC (Figure 4F).

3.5. RuC increases the levels of pyruvate and lactate

Considering that the significant inhibition of respiration may result in activation of the glycolytic pathway, the levels of pyruvate and lactate that were released by HepG2 and HeLa cells were also measured. The effects of RuC (100 nmol/L) were more pronounced than cisplatin, increasing the levels of both pyruvate (116% and 72%; Figure 5A, B) and lactate (60% and 42%; Figure 5C, D) in HepG2 and HeLa cells, respectively. Cisplatin did not alter the levels of pyruvate or lactate in HeLa cells (Figure 5B, D). In HepG2 cells, cisplatin (10 nmol/L) increased pyruvate levels (55%; Figure 5A), but it did not affect lactate levels (Figure 5C).

3.6. Recovery curve of HepG2 and HeLa cells

HepG2 cells did not recover their proliferation capacity after treatment with RuC or the highest concentration of cisplatin for 9 days in standard culture media (Figure 6A, C). Similarly, the proliferation of HeLa cells was impaired after cisplatin treatment. After treatment with RuC, these cells partially recovered their proliferation capacity, but the number of cells was less than in the absence of the compound (control; Figure 6B, D). Additionally, 100 nmol/L cisplatin, corresponding to the highest concentration of RuC, was less efficient to inhibit the cell growth of either cell lineage (Figure 6A, B, C, D).

4. Discussion

Innovative anticancer drugs with new molecular mechanisms of action are essential for the chemotherapeutic treatment of specific types of cancer to overcome the toxic effects and chemoresistance of the currently available compounds. The organometallic compound RuC (Figure 1) is a potential novel therapy for the treatment of HCC and cervical adenocarcinoma. The toxicity screening of RuC showed that HepG2 and HeLa cells were sensitive cell lines over 48 and 72 h of exposure (Table 1, Supplementary Table S2). In all of the experiments, the metallic chemotherapeutic drug cisplatin was used as a positive control because it has been used for the treatment of HCC [31, 32] and cervical tumors [33, 34]. After 48 h of drug exposure, RuC was cytotoxic in HepG2 and HeLa cells at nanomolar concentrations, whereas cisplatin had similar cytotoxicity in the micromolar range (Figure 2), thus indicating the higher *in vitro* potency of RuC against HepG2 and HeLa cells compared with cisplatin. This pattern was observed in all of the assays (MTT, crystal violet, and neutral red assays). Our results corroborate previous studies that investigated other Ru compounds and reported antineoplastic effects *in vitro*, such as Ru(II) complexes with a chloro-substituted phenylazopyridine ligand [35], 2-nitroimidazole-Ru polypyridyl [36], Ru(II)-thymine [37], and dimeric kaempferol-Ru [38] complexes.

With regard to metal drugs, cisplatin has been used in several protocols for the treatment of cancer. More recently, other drugs, such as carboplatin, oxaliplatin, heptaplatin, lobaplatin, nedaplatin, and dicyclopatin, have been approved as antineoplastic drugs in different countries [39]. Although platinum anticancer drugs are used as a component of nearly 50% of all cancer treatments and other metal compounds have been developed [39], NKP-1339 is the only Ru compound that is currently in clinical trial with patients with advanced solid tumors (NCT01415297) [40]. We previously demonstrated that RuC has antitumor effects in Walker-256 tumor-bearing rats, without inducing side effects after 2 weeks of systemic treatment [14]. In the present study, we observed its *in vitro* effect against HepG2 and HeLa cells, suggesting that RuC may be a potential candidate for clinical studies of hepatocarcinoma and cervical adenocarcinoma.

The effects of RuC on both cell lines may be associated with the reduction of cell proliferation that was observed at the highest concentration of the compound (Figure 3). The higher cytotoxicity of RuC compared with cisplatin may result from metal that is released from the complex, which is favored by the acidic environment of tumor cells. Thus, we evaluated the influence of RuC on the rates of lactate and pyruvate release, which can reduce cellular pH. The results showed that RuC increased the levels of pyruvate and lactate in both cell lines, whereas cisplatin increased only pyruvate levels at the highest concentration (10 μmol/L) in HepG2 cells. The higher levels of lactate and pyruvate in HepG2 cells that were treated with RuC lowered cellular pH and may suggest the activation of glycolysis, possibly as a compensatory response to the strong inhibition of oxidative phosphorylation by the

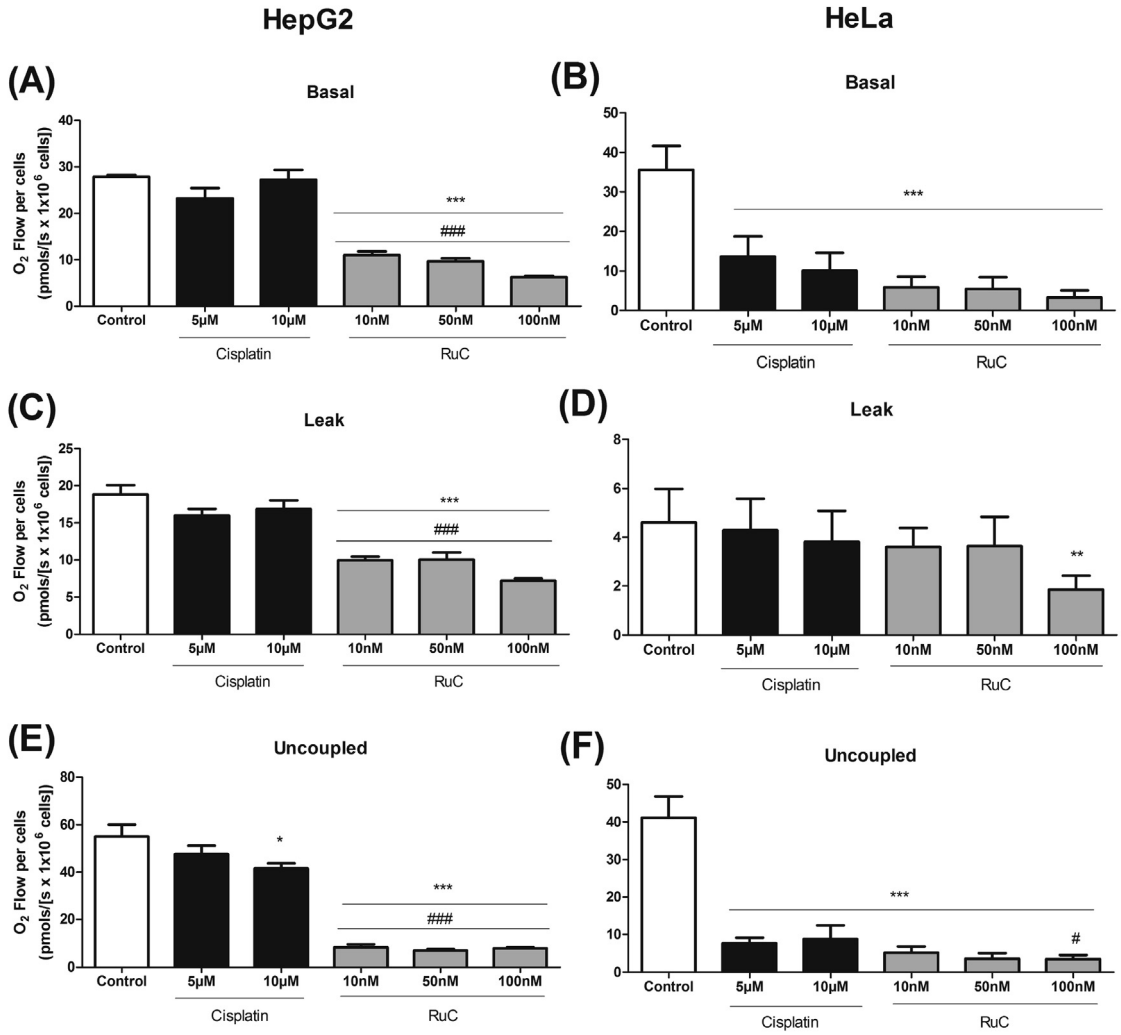

Figure 4. Effect of cisplatin and RuC on the respiration of HepG2 cells (A, C, E) and HeLa cells (B, D, F). The experimental conditions are described in the Materials and Methods. Briefly, cells (10^6 cells/well) were seeded in 60 mm plates for 48 h, treated, and transferred to Oroboros 2-K oxygraph chambers where oxygen consumption was determined in the absence of inhibitors or uncouplers (basal state), in the presence of oligomycin (leak state), and in the presence of FCCP (uncoupled state). The results are expressed as respiration ($pmolO_2/1 \times 10^6$ cells) relative to the control. The values are expressed as the mean ± SEM of four independent experiments each in quadruplicate; n = 16. $^{*}p < 0.05$, $^{**}p < 0.01$, $^{***}p < 0.001$, significantly different from control (0.1% DMSO [vehicle]); $^{\#}p < 0.05$, $^{\#\#}p < 0.01$, $^{\#\#\#}p < 0.001$, significantly different from 10 μmol/L cisplatin.

compound. These results are consistent with the respiration assays, in which the effects of RuC were more pronounced than cisplatin on both cell lines. However, RuC at intermediate concentrations (10 and 50 nmol/L) significantly inhibited the leak state only in HepG2 cells. Oxygen consumption during the leak state depends on the integrity of the inner mitochondrial membrane, suggesting that RuC affects the membrane permeability of distinct pathways in HepG2 and HeLa cells. These results suggest that the impairment of oxidative phosphorylation that was induced by RuC may be one mechanism of its pronounced cytotoxicity. These results are consistent with our previous data in Walker-256 ascitic tumor cells, in which RuC inhibited the respiration [14].

The activation of mitochondrial signaling pathways and modulation of mitochondrial physiology may circumvent the drug-resistant phenotype of cancer cells [41, 42, 43]. Several experimental drugs have also been reported to act primarily on mitochondria to induce cancer cell death [42, 44]. The modulation of key enzymes that are involved in the energetic metabolism of cancer cells, such as lactate dehydrogenase (LDH), hexokinase II (HK-II), and 6-phosphofructo-1-kinase (PFK-1) [45], may compromise cellular bioenergetics, leading to the loss of membrane integrity, the loss of recovery capacity, and ultimately cell death as apoptosis/necrosis [46]. Tumor necrosis was reported previously in Walker-256 cells in tumor-bearing rats that were treated with RuC (10 mg/kg, i.p.) [14].

Interestingly, the severity of the effects of RuC on HepG2 cells prevented the cells from recovering (Figure 6), which was not observed in HeLa cells at the same concentration of RuC (100 nmol/L). HepG2 cells were more affected by RuC than HeLa cells. This may be related to resistance mechanisms of HeLa cells that involve the higher expression of certain proteins, such as Herpud1 (i.e., a mammalian ubiquitin domain protein that is strongly induced by the unfolded protein response) [47]. The function of Herpud1 is not fully understood, but evidence suggests that it appears to have a cytoprotective function, conferring resistance to endoplasmic reticulum stress in HeLa cells [48] and resistance to autophagy in cancer cells [49]. The inhibition of respiration is well known to be associated with an increase in ROS levels and consequently conditions of oxidative stress [50, 51]. We recently found that RuC modulates oxidative stress in Walker-256 cells [14]. In this study, RuC inhibited the respiration of both HepG2 and HeLa cell lines, but only HeLa cells partially recovered their proliferation capacity. These results indicate that different cancer cells have distinct sensitivities to chemotherapies,

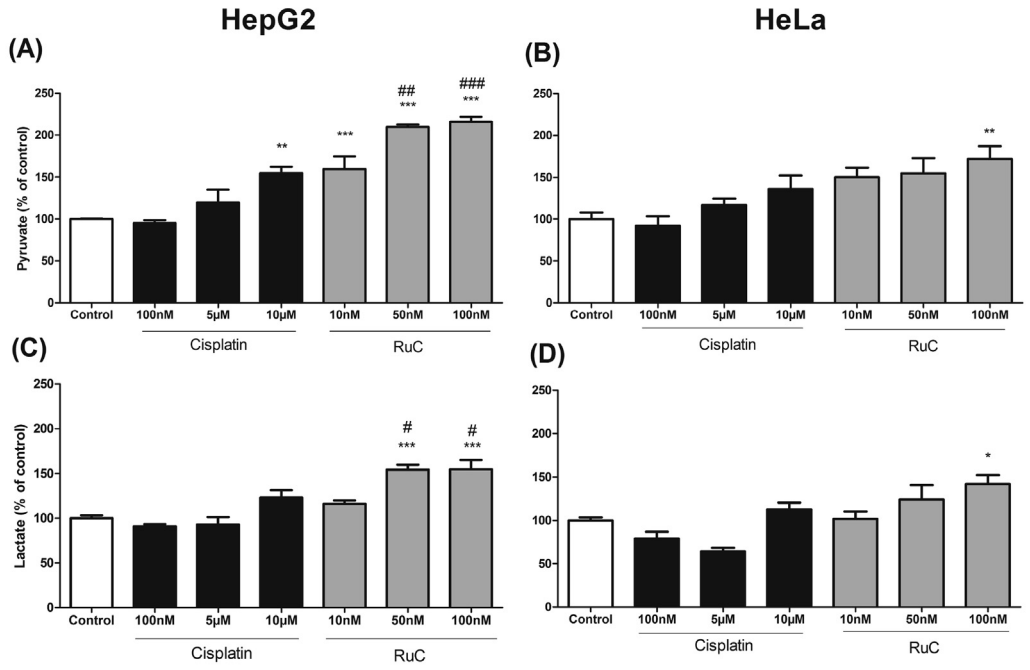

Figure 5. Levels of pyruvate (A, B) and lactate (C, D) released by HepG2 and HeLa cells that were treated with cisplatin or RuC. The experimental conditions are described in the Materials and Methods. The cells (10^6 cells/well) were seeded in 60 mm plates and treated with cisplatin (5 and 10 μmol/L) and RuC (10, 50, and 100 nmol/L) for 48 h. Pyruvate and lactate concentrations were measured in the culture medium. The results are expressed as the mean ± SEM of four independent experiments each in quadruplicate; n = 16. $^{*}p < 0.05$, $^{**}p < 0.01$, $^{***}p < 0.001$, significantly different from control (0.1% DMSO [vehicle]); $^{\#}p < 0.05$, $^{\#\#}p < 0.01$, $^{\#\#\#}p < 0.001$, significantly different from 10 μmol/L cisplatin.

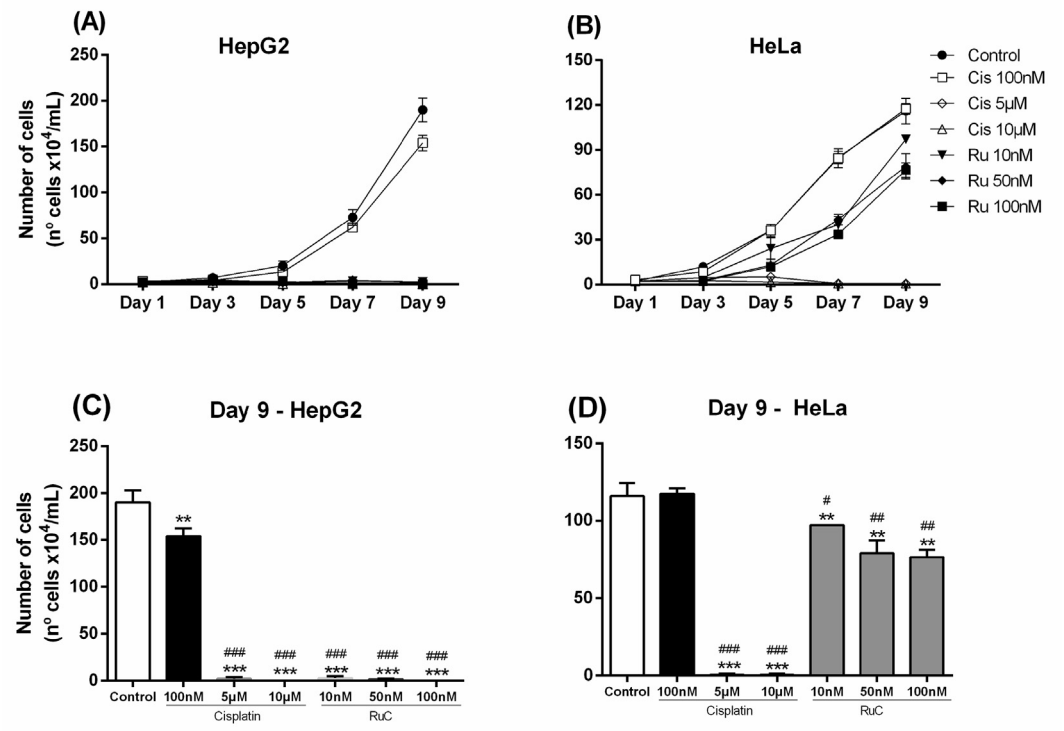

Figure 6. Time course of recovery proliferation curves of HepG2 (A and HeLa (B) cells and number of viable cells at the 9th day (C, D. The experimental conditions are described in the Materials and Methods. The cells (10^6 cells/well) were plated in six-well plates at a cell density of 1.5×10^4 and treated with cisplatin or RuC during the first 48 h of the experiment protocol. After treatment, cell proliferation was monitored for 9 days. The Trypan blue results are expressed as the number of cells (n° of cells $\times 10^4$/mL) of 2 independent experiments each in quadruplicate; n = 8. The statistic comparisons at the 9th day were calculated by one-way ANOVA followed by the Tukey test. $^{**}p < 0.01$, $^{***}p < 0.001$, significantly different from control (0.1% DMSO [vehicle]); $^{\#}p < 0.05$, $^{\#\#}p < 0.01$, $^{\#\#\#}p < 0.001$, significantly different from 100 nmol/L cisplatin.

thus justifying further studies that investigate cellular responses and resistance to anticancer treatments.

The current standard treatment of cervical adenocarcinoma consists of radical surgery and platinum-based chemotherapy. The average 5-year survival rate of cervical cancer has reached 66% in developed countries, but less than half of patients from developing countries survive longer than 5 years [52, 53]. The traditional therapies for HCC, such as resection, transplantation, and transarterial interventions, have limited efficacy, and the available drugs may also affect non-tumor cells, resulting in serious side effects [54, 55]. Sorafenib is the first-line chemotherapeutic drug in patients with advanced HCC, but it has a high rate of resistance that occurs through several mechanisms [56, 57], which significantly limits its beneficial effects. The present results showed that RuC was more effective than cisplatin in both HepG2 and HeLa cells, particularly HepG2 cells. This antineoplastic effect appeared to be related to the impairment of oxidative phosphorylation and activation of the glycolysis pathway. The failure of hepatocarcinoma cells to recover demonstrates the significant toxicity of RuC in these cells. Our findings may encourage further *in vitro* and *in vivo* investigations of the potential of this compound for the treatment for hepatocarcinoma.

Declarations

Author contribution statement

Carlos Eduardo Alves de Souza: Conceived and designed the experiments; Performed the experiments; Analyzed and interpreted the data; Contributed reagents, materials, analysis tools or data; Wrote the paper.

Amanda do Rocio Andrade Pires: Performed the experiments.

Carolina Riverin Cardoso, Rose Maria Carlos: Contributed reagents, materials, analysis tools or data.

Silvia Maria Suter Correia Cadena: Conceived and designed the experiments; Analyzed and interpreted the data; Contributed reagents, materials, analysis tools or data; Wrote the paper.

Alexandra Acco: Analyzed and interpreted the data; Contributed reagents, materials, analysis tools or data; Wrote the paper.

Funding statement

This work was supported by Conselho Nacional de Desenvolvimento Científico e Tecnológico [CNPq, Brazil, Grant 307977/2015-3]. CEAS and CRC are recipients of a graduate fellowship from Coordenação de Aperfeiçoamento de Pessoal de Nível Superior [CAPES, Brazil, Financial code 001]. AA and SMSCC are recipients of a research fellowship (PQ 2) from CNPq.

Competing interest statement

The authors declare no conflict of interest.

Additional information

Supplementary content related to this article has been published online at https://doi.org/10.1016/j.heliyon.2020.e03862.

Acknowledgements

We thank Dr. Anderson Joel Martino Andrade for helping in statistical analysis.

References

[1] World Health Organization, Cancer tomorrow. https://gco.iarc.fr/tomorrow/home. (Accessed April 2020).
[2] S.H. Van Rijt, P.J. Sadler, Current applications and future potential for bioinorganic chemistry in the development of anticancer drugs, Drug Discov. Today 14 (2009) 1089–1097.
[3] L.H. Einhom, J. Donohue, Cis-diamminedichloro-platinum, vinblastine, and bleomycin combination chemotherapy in disseminated testicular cancer, Ann. Intern. Med. 87 (1977) 293–298.
[4] S. Dasari, P.B. Tchounwou, Cisplatin in cancer therapy: molecular mechanisms of action, Eur. J. Pharmacol. 5 (2014) 740, 364-78.
[5] L. Galluzzi, L. Senovilla, I. Vitale, Molecular mechanisms of cisplatin resistance, Oncogene 12 (3) (2012) 1869–1883.
[6] M.A. Jakupec, E. Reisner, A. Eichinger, et al., Redox-active antineoplastic ruthenium complexes with indazole: correlation of in vitro potency and reduction potential, J. Med. Chem. 48 (2005) 2831–2837.
[7] E. Reisner, V.B. Arion, M.F.C.G. Da Silva, et al., Tuning of redox potentials for the design of ruthenium anticancer drugs - an electrochemical study of [trans-RuCl4L(DMSO)]− and [trans-RuCl4L2]− complexes, where L = imidazole, 1,2,4-triazole, indazole, Inorg. Chem. 43 (2004) 7083–7093.
[8] E. Reisner, V.B. Arion, A. Eichinger, et al., Tuning of redox properties for the design of ruthenium anticancer drugs: Part 2. Syntheses, crystal structures, and electrochemistry of potentially antitumor [RuIII/IICl6-n(azole)n]z (n = 3, 4, 6) complexes, Inorg. Chem. 44 (2005) 6704–6716.
[9] R.L.S.R. Santos, R. Van Eldik, D. De Oliveira Silva, Kinetic and mechanistic studies on reactions of diruthenium(II,III) with biologically relevant reducing agents, Dalton Trans. 42 (2013) 16796–16805.
[10] M.J. Clarke, V.M. Bailey, P.E. Doan, et al., 1H NMR, EPR, UV−vis, and electrochemical studies of imidazole complexes of Ru(III). Crystal Structures of cis-$[(Im)_2(NH_3)_4RuIII]Br_3$ and $[(1MeIm)_6RuII]Cl_2{\cdot}2H_2O$, Inorg. Chem. 35 (1996) 4896–4903.
[11] M. Hartmann, K.G. Lipponer, B.K. Keppler, Imidazole release from the antitumor-active ruthenium complex imidazolium transtetrachlorobis (imidazole) ruthenate(III) by biologically occurring nucleophiles, Inorg. Chem. Acta 267 (1998) 137–141.
[12] D.R. Frasca, M.J. Clarke, Alterations in the binding of $[Cl(NH_3)5RuIII]^{2+}$ to DNA by glutathione: reduction, autoxidation, coordination, and decomposition, J. Am. Chem. Soc. 121 (1999) 8523–8532.
[13] C.R. Cardoso, M.V.S. Lima, J. Chelesk, et al., Luminescent ruthenium complexes for theranostic applications, J. Med. Chem. 57 (2014) 4906–4915.
[14] C.E. Alves De Souza, H.M. Alves De Souza, M.C. Stipp, et al., Ruthenium complex exerts antineoplastic effects that are mediated by oxidative stress without inducing toxicity in Walker-256 tumor-bearing rats, Free Radic. Biol. Med. 110 (2017) 228–239.
[15] O. Warburg, On the origin of cancer cells, Science 123 (1956) 309–314.
[16] C.H. Tsai, A.C. Hung, Y.Y. Chen, et al., 3'-hydroxy-4'-methoxy-β-methyl-β-nitrostyrene inhibits tumorigenesis in colorectal cancer cells through ROS-mediated DNA damage and mitochondrial dysfunction, Oncotarget 8 (11) (2017) 18106–18117.
[17] M. Comelli, I. Pretis, A. Buso, et al., Mitochondrial energy metabolism and signalling in human glioblastoma cell lines with different PTEN gene status, J. Bioenerg. Biomembr. 50 (1) (2018) 33–52.
[18] S.L. Chan, W. Fu, P. Zhang, et al., Herp stabilizes neuronal Ca^{2+} homeostasis and mitochondrial function during endoplasmic reticulum stress, J. Biol. Chem. 279 (2004) 28733–28743.
[19] T. Mossman, Rapid colorimetric assay for cellular growth and survival: application to proliferation and cytotoxicity assays, J. Immunol. Methods 65 (55–63) (1983).
[20] A.D.R.A. Pires, A.C. Ruthes, S.M. Cadena, et al., Cytotoxic effect of *Agaricus bisporus* and *Lactarius rufus* β-D-glucans on HepG2 cells, Int. J. Biol. Macromol. 58 (2013) 95–103.
[21] R.J. Gillies, N. Didier, M. Denton, Determination of cell number in monolayer cultures, Anal. Biochem. 159 (1986) 109–113.
[22] E. Borenfreund, J. Puerner, A simple quantitative procedure using monolayer cultures for cytotoxicity assays (HTD/NR-90), J. Tissue Cult. Methods 9 (7–9) (1984).
[23] W. Strober, Current protocols in immunology trypan blue exclusion test of cell viability, Curr. Protoc. Immunol. 2 (2015) 1–3.
[24] E. Gnaiger, Bioenergetics at low oxygen: dependence of respiration and phosphorylation on oxygen and adenosine diphosphate supply, Respir. Physiol. 128 (2001) 277–297.
[25] E. Hutter, et al., High-resolution respirometry - a modern tool in aging research, Exp. Gerontol. 41 (2006) 103–109.
[26] K. Renner, A. Amberger, G. Konwalinka, et al., Changes of mitochondrial respiration, mitochondrial content and cell size after induction of apoptosis in leukemia cells, Biochim. Biophys. Acta 1642 (2003) 115–123.
[27] E. Gnaiger, Capacity of oxidative phosphorylation in human skeletal muscle: new perspectives of mitochondrial physiology, Int. J. Biochem. Cell Biol. 41 (2009) 1837–1845.
[28] R.L. Czoc, W. Lamprech, Pyruvate, Phosphoenolpyruvate and D-Glycerate-2-Phosfate, Methods Enzym. Anal. (1974) 1446–1451. Edited by Bergmeyer HU. Weinheim.
[29] I. Gutmann, W.A. Wahlefeld, L-(+)-Lactate determination with lactate dehydrogenase and NAD, Methods Enzym. Anal. (1974) 1464–1469. Edited by Bergmeyer HU. Weinheim.
[30] M.M. Bradford, A rapid and sensitive method for the quantitation of microgram quantities of protein utilizing the principle of protein-dye binding, Anal. Biochem. 72 (1976) 248–254.
[31] J.K. Kim, J.W. Kim, I.J. Lee, et al., Factors affecting survival after concurrent chemoradiation therapy for advanced hepatocellular carcinoma: a retrospective study, Radiat. Oncol. 12 (1) (2017) 133.

[32] K. Ogawa, K. Kamimura, Y. Watanabe, et al., Effect of double platinum agents, combination of miriplatin-transarterial oily chemoembolization and cisplatin-hepatic arterial infusion chemotherapy, in patients with hepatocellular carcinoma: report of two cases, World J. Clin. Cases 5 (6) (2017) 238–246.
[33] N.R. Datta, E. Stutz, M. Liu, et al., Concurrent chemoradiotherapy vs. radiotherapy alone in locally advanced cervix cancer: a systematic review and meta-analysis, Gynecol. Oncol. 145 (2) (2017) 374–385.
[34] W. Small JR., M.A. Bacon, A. Bajaj, et al., Cervical cancer: a global health crisis, Cancer 123 (13) (2017) 2404–2412.
[35] T. Nhukeaw, P. Temboot, K. Hansongnern, A. Ratanaphan, Cellular responses of BRCA1-defective and triple-negative breast cancer cells and in vitro BRCA1 interactions induced by metallo-intercalator ruthenium(II) complexes containing chloro-substituted phenylazopyridine, BMC Cancer 14 (2014) 73.
[36] O. Mazuryk, K. Magiera, B. Rys, et al., Multifaceted interplay between lipophilicity, protein interaction and luminescence parameters of non-intercalative ruthenium(II) polypyridyl complexes controlling cellular imaging and cytotoxic properties, J. Biol. Inorg. Chem. 19 (2014) 1305–1316.
[37] K.M. Oliveira, L.D. Liany, R.S. Corrêa, et al., Selective Ru(II)/lawsone complexes inhibiting tumor cell growth by apoptosis, J. Inorg. Biochem. 176 (2017) 66–76.
[38] P. Thangavel, B. Viswanath, S. Kim, Synthesis and characterization of kaempferol-based ruthenium (II) complex: a facile approach for superior anticancer application, Mater. Sci. Eng. C Mater. Biol. Appl. 1 (89) (2018) 87–94.
[39] N.P. Barry, P.J. Sadler, Exploration of the medical periodic table: towards new targets, Chem. Commun. 49 (2013) 51064, 1089–1097.
[40] NCT01415297, Dose escalation study of NKP-1339 to treat advanced solid tumors. Clinical trials. https://clinicaltrials.gov/ct2/show/study/NCT01415297?term=NKP-1339&rank=1 (Accessed April 2020).
[41] A. Lyakhovich, M.E. Lleonart, Bypassing mechanisms of mitochondria-mediated cancer stem cells resistance to chemo- and radiotherapy, Oxid. Med. Cell Longev. (2016) 1716341.
[42] M. Esner, D. Graifer, M.E. Lleonart, et al., Targeting cancer cells through antibiotics-induced mitochondrial dysfunction requires autophagy inhibition, Cancer Lett 384 (2017) 60–69.
[43] A.S. Tan, J.W. Baty, L.F. Dong, et al., Mitochondrial genome acquisition restores respiratory function and tumorigenic potential of cancer cells without mitochondrial DNA, Cell Metabol. 6 (21) (2015) 81–94.
[44] Y. Lu, J. Kwintkiewicz, Y. Liu, et al., Chemosensitivity of IDH1-mutated gliomas due to an impairment in PARP1-mediated DNA repair, Cancer Res. 1 (77) (2017) 1709–1718.
[45] W. Zhu, L. Ye, J. Zhang, et al., PFK15, a small molecule inhibitor of PFKFB3, induces cell cycle arrest, apoptosis and inhibits invasion in gastric cancer, PloS One 26 (11) (2016), e0163768.
[46] R.R. Mallepally, N. Chintakuntla, V.R. Putta, et al., Synthesis, spectral properties and DFT calculations of new ruthenium (II) polypyridyl complexes; DNA binding affinity and in vitro cytotoxicity activity, J. Fluoresc. 22 (2017).
[47] K. Kokame, K.L. Agarwala, H. Kato, T. Miyata, Herp, a new ubiquitin-like membrane protein induced by endoplasmic reticulum stress, J. Biol. Chem. 275 (2000) 32846–32853.
[48] F. Paredes, A.V. Parr, N. Torrealba, et al., HERPUD1 protects against oxidative stress-induced apoptosis through downregulation of the inositol 1,4,5-trisphosphate receptor, Free Radic. Biol. Med. 90 (2016) 206–218.
[49] C. Quiroga, D. Gatica, F. Paredes, et al., Herp depletion protects from protein aggregation by upregulating autophagy, Biochim. Biophys. Acta 1833 (2013) 3295–3305.
[50] B.J. Berry, A.J. Trewin, A.M. Amitrano, Use the protonmotive force: mitochondrial uncoupling and reactive oxygen species, J. Mol. Biol. (2018). S0022–2836; 30176-1.
[51] M.P. Murphy, How mitochondria produce reactive oxygen species, Biochem. J. 417 (2009) 1–13.
[52] E.L. Franco, N.F. Schlecht, D. Saslow, The epidemiology of cervical cancer, Cancer J. 9 (2003) 348–359.
[53] L. Chang, R. Guo, Comparison of the efficacy among multiple chemotherapeutic interventions combined with radiation therapy for patients with cervix cancer after surgery: a network meta-analysis, Oncotarget 8 (30) (2017) 49515–49533.
[54] R. Masuzaki, M. Omata, Treatment of hepatocellular carcinoma, Indian J. Gastroenterol. 27 (3) (2008) 113–122.
[55] G. Baffy, Decoding multifocal hepatocellular carcinoma: an opportune pursuit, Hepatobiliary Surg. Nutr. 4 (2015) 206–210.
[56] L. Niu, L. Liu, S. Yang, et al., New insights into sorafenib resistance in hepatocellular carcinoma: responsible mechanisms and promising strategies, Biochim. Biophys. Acta 17 (2017) pii: S0304-419; (17); 30140-30143.
[57] J. Chen, R. Jin, J. Zhao, et al., Potential molecular, cellular and microenvironmental mechanism of sorafenib resistance in hepatocellular carcinoma, Cancer Lett. 367 (1) (2015) 1–11. Epub 2015 Jul 10.